ISBN: 978-3-95450-261-5 ISSN: 2673-7000 doi: 10.18429/JACoW-NAPAC2025-THP091

TUNING OF A FORCE-NEUTRAL ADJUSTABLE-PHASE UNDULATOR*

M. Qian†, Y. Piao, J. Xu
Argonne National Laboratory, Lemont, IL, USA

Abstract

We present tuning experiences for trajectory and phase error correction in a hybrid permanent magnet-based adjustable-phase undulator (APU). The APU, which we developed, features a period length of 17.2 mm, an effective field of 0.55 T, a gap of 8.5 mm, and a total length of 2.4 m. This planarly polarized undulator adjusts field intensity through the longitudinal movement of magnet arrays, with mechanically linked additional magnet arrays for force compensation. The focus of this report is on the tuning methods, which our engineering experience demonstrates to be highly effective in optimizing the performance of this type of undulator.

INTRODUCTION

Adjustable-phase undulators (APUs) offer several advantages over traditional adjustable-gap undulator (AGU) designs. By enabling phase tuning through small, low-inertia displacements, APUs allow for much faster spectral or polarization switching, which is especially valuable in time-resolved experiments. Their compact mechanical structure—free from large vertical motions—not only simplifies integration but also enhances robustness. In addition, the reduced number of moving components improves mechanical reliability and long-term stability, while lowering maintenance demands [1].

While most previously constructed APUs have been based on pure permanent magnet designs [2], the Advanced Photon Source (APS) has initiated the development of hybrid-type APUs that incorporate ferromagnetic materials to enhance performance and flexibility. The long-term goal is to demonstrate the feasibility of hosting multiple APU arrays within a highly constrained footprint [3].

APU17.2 (Fig. 1) is the second hybrid-type, permanent magnet-based APU developed at APS, which reuses the magnet arrays from a legacy planar undulator. The original device is of the AGU type with a minimum magnetic gap of 11.5 mm. In the current APU17.2 configuration, the device is designed as an out-of-vacuum system with a fixed magnetic gap of 8.5 mm. It features a period length of 17.2 mm, an effective field of 0.55 T, and a total length of 2.4 m.

To mitigate strong vertical and longitudinal magnetic forces, a force-compensation magnet array was incorporated. This reduced the magnetic force per period from approximately 34 N to about 2 N, significantly lowering the mechanical load and improving stability. The APU17.2 is actuated along a single axis using a servo motor with a resolver for commutation. High-precision position control is achieved by directly servoing the motor with feedback from a linear encoder, providing accurate and repeatable motion across the tuning range. This device has been fabricated and tuned. During its development, new insights were gained—particularly regarding electron trajectory correction and phase error tuning—which are presented in this report.

Figure 1: Photo of APU17.2 during magnetic measurement.

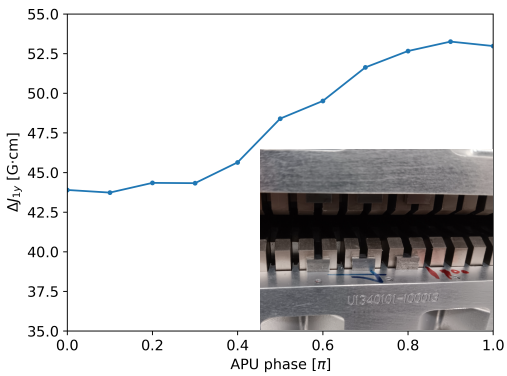

Figure 2: Trajectory signatures of a pair of side shims measured using a long flipping coil. The embedded panel in the bottom right illustrates the side shims attached to the undulator magnet arrays.

TRAJECTORY TUNING

Trajectory straightness is critical for undulator performance, as deviations can degrade the quality of the emitted radiation. In the case of APU17.2, trajectory tuning is accomplished using iron shims, similar to the side shims employed at the APS [4]. We identified a shim geometry that remains stable across all undulator phases without requiring additional measures to secure the shims. The trajectory signatures, defined as the integrated dipole field of the shims, were measured and found to be effective across all APU phases, as shown in Fig. 2. This configuration shows stronger integrated fields at larger APU phases (smaller K), unlike AGUs where shim effects weaken at low K.

* Work supported by the U.S. DOE Office of Science, Office of Basic Energy Sciences, under Contract No. DE-AC02-06CH11357.
† mqian@anl.gov

ISBN: 978-3-95450-261-5 ISSN: 2673-7000 doi: 10.18429/JACoW-NAPAC2025-THP091

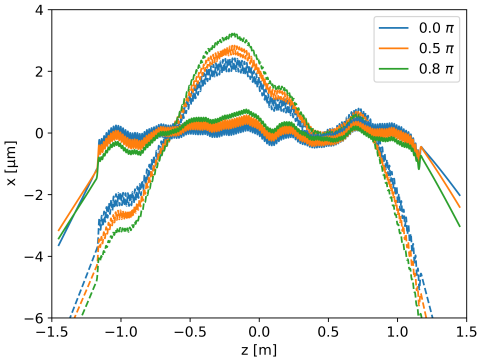

Figure 3: Trajectories before correction (dashed lines) and after correction (solid lines) using side shims. The APU phase for each measurement is indicated in the legend.

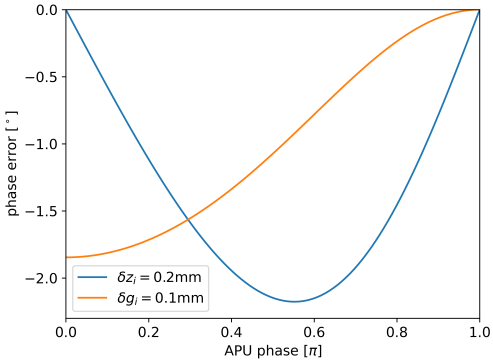

Figure 4: Phase error over a pole (half period) when a section of the magnet array is displaced by 0.2 mm in the longitudinal direction (blue) or the gap is offset by 0.1 mm (yellow).

To direct the trajectory corrections, we employed the same differential evolution algorithm-based optimization method developed at APS [5], assigning higher weights to cases with large undulator K. The resulting shim map consists of 16 locations for shim placement. At each location, two shims are installed on the outer sides of the bottom and top magnet arrays to cancel the horizontal field. The improvement achieved is demonstrated in Fig. 3, which presents trajectories at three different APU phases. The trajectory deviation was reduced from ± 3 m to ± 0.5 m, significantly enhancing straightness. These straightened trajectories provide a foundation for subsequent phase error tuning.

PHASE ERROR REDUCTION

When the undulator trajectory is tuned straight and the deviation is small enough, the phase error is mainly caused by local undulator K variation. Based on the undulator wavelength equation, the phase error over one pole could be expressed as:

$$\delta\phi_i = \pi \frac{2\bar{K}}{2+\bar{K}^2}\delta K_i \,, \tag{1}$$

where $\delta\phi_i$ is the phase error over the i-th pole, $\bar{K}$ is the mean undulator K of the device, and δK_i is the local undulator K difference from the mean at that pole.

The field in the mid-plane generated by an APU magnet array is:

$$B_y = B_0 \cos\left(\frac{2\pi(z-z')}{\lambda_u}\right)\exp\left(-\frac{2\pi y'}{\lambda_u}\right) . \tag{2}$$

Here, λ_u is the undulator period length, z is the longitudinal coordinate, z' is the longitudinal position of the array, and y' is the distance from the mid-plane to the surface of the magnet array. For simplicity, higher harmonics of the magnetic field are neglected. The B_z component is not considered, as it has no significant effect in planar APU devices.

An important source of phase error, as in the case of AGUs, is the gap error. By superimposing the contributions from the two APU magnet arrays with a local gap error, we obtain:

$$\delta\phi_i = -\pi^2 \frac{2\bar{K}_\Phi^2}{2+\bar{K}_\Phi^2}\frac{\delta g_i}{\lambda_u} \,, \tag{3}$$

where δg_i is the local gap error at the location of the i-th pole. In this case $\bar{K}_\Phi = K_0\cos(\Phi/2)$, where K_0 is the undulator K value of the in-phase situation; Φ is the APU phase defined as $2\pi\Delta z'/\lambda_u$; and $\Delta z'$ is the longitudinal position difference between the moving magnet array and the fixed (reference) one. Since the gap variation term is independent of the undulator phase shift, the same phase error-gap relationship holds as in the AGU cases.

Each APU17.2 magnet array is mechanically mounted on three holders, forming three longitudinal sections with a similar number of poles. Initially, these sections may not be precisely aligned, leading to local variations in the undulator parameter K and resulting phase errors. If, in a localized region, there is a longitudinal displacement of the moving array—corresponding to an APU phase difference $\delta\Phi_i$—the local magnetic field will differ from that in the rest of the undulator by:

$$\begin{aligned}\delta K_i &= K_0\cos(\Phi/2+\delta\Phi_i/2) - \bar{K} \\ &\approx -\bar{K}_\Phi \tan(\Phi/2)\delta\Phi_i/2 \,.\end{aligned} \tag{4}$$

so that the phase error over this pole in this case is:

$$\delta\phi_i = -\pi\frac{\bar{K}_\Phi^2}{2+\bar{K}_\Phi^2}\delta\Phi_i\tan(\Phi) \,. \tag{5}$$

The phase errors arising from gap errors and sectional positioning errors, as described by Eq. (3) and Eq. (5), are quantified for APU17.2 in Fig. 4. The effect of gap errors peaks at the in-phase condition, while the impact of sectional positioning errors—unique to APUs—peaks around 0.55 π for this device. Since these two effects behave differently, it is essential to correct both types of errors. A least-squares method, combined with the data in Fig. 4, was used to predict the necessary adjustments for correcting both errors based on measured phase error. Gap errors were addressed by placing shims between the frame and the magnet array,

ISBN: 978-3-95450-261-5 ISSN: 2673-7000 doi: 10.18429/JACoW-NAPAC2025-THP091

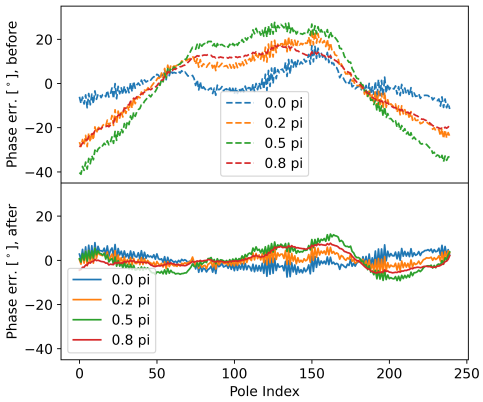

Figure 5: The top panel shows phase error at four APU phases before tuning; the bottom panel shows the error after tuning. Both use the same scale for direct comparison.

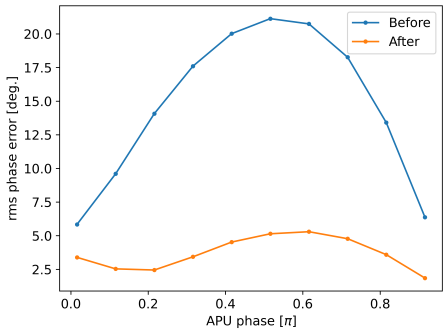

Figure 6: RMS phase error before and after tuning.

while sectional positioning errors were corrected by inserting shims between neighboring sections. The final results show that the phase error is significantly reduced. The tuned phase error is presented in Fig. 5, and the corresponding rms phase error is shown in Fig. 6.

Even though the sectional z-misalignment has been minimized, small-scale localized z-misalignments remain. At intermediate undulator K values, the phase error is particularly sensitive to these misalignments, as illustrated by Fig. 5, resulting in a slightly increased phase error under these conditions.

MECHANICAL STABILITY OF MAGNET ARRAYS

Despite force compensation, the poles in the undulator magnet arrays still experience full-strength internal longitudinal forces. The magnet arrays were repurposed from an AGU, where longitudinal forces are absent, so the original design did not account for longitudinal stability of the poles.

We observed changes of up to 3 G in the effective field due to mechanical variations, as shown in Fig. 7. Measurements at an APU phase of 0.5π—where longitudinal forces on the poles are greatest—were taken after several hours of stabilization at 0π. The system requires several hours to stabilize as longitudinal forces induce pole motion, resisted by friction. Analysis of different sections revealed that section 1 was more stable, with field changes under 1 G, while sections 2 and 3 showed larger variations of 3–4 G, indicating variability in longitudinal stability. To improve stability in future designs, additional holders will be used to better secure the poles, and the vertical dimensions of the poles and magnets will be reduced.

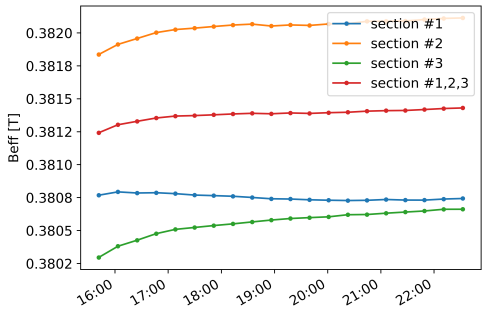

Figure 7: Effective field (B_{eff}) of the full device and different sections over time.

CONCLUSION

The APU17.2 has been built and successfully tuned. We demonstrate that the use of side shims, in combination with the differential evolution-based optimization method developed for adjustable-gap undulators (AGUs) at APS, is effective for trajectory tuning of hybrid-type adjustable-phase undulators (APUs). Phase error correction was achieved by mechanically shimming the magnet array gap and adjusting the longitudinal positions of the array sections. The reused legacy AGU magnet arrays are multi-sectional, requiring this section gap re-adjustment. Precise longitudinal alignment is critical for minimizing phase errors, and future single-section designs will help improve performance.

REFERENCES

[1] J. Z. Xu *et al.*, "A force-neutral adjustable phase undulator for a compact x-ray FEL," *J. Phys. Conf. Ser.*, vol. 2687, no. 3, p. 032017, 2024. doi:10.1088/1742-6596/2687/3/032017

[2] A. Temnykh *et al.*, "CHESS upgrade with compact undulator magnets: Operating experience and first results," *AIP Conf. Proc.*, vol. 1741, p. 020003, 2016. doi:10.1063/1.4952782

[3] J. Z. Xu *et al.*, "Force-neutral adjustable phase undulator," in *Proc. IPAC'24*, Nashville, TN, USA, May 2024, pp. 1369–1372. doi:10.18429/JACoW-IPAC2024-TUPG55

[4] Y. Piao *et al.*, "Magnetic shims studies for APS-U hybrid permanent magnet undulators," in *Proc. IPAC'21*, Campinas, Brazil, May 2021, pp. 3941–3944. doi:10.18429/JACoW-IPAC2021-THPAB077

[5] M. Qian *et al.*, "Experience with algorithm-guided tuning of APS-U undulators," in *Proc. IPAC'21*, Campinas, Brazil, May 2021, pp. 2915–2917. doi:10.18429/JACoW-IPAC2021-WEPAB130